Empirical approach to the description of spectral performance degradation of silicon photodiodes used as particle detectors

G. Kalinka [a,*], M. Novák [a], A. Simon [a], Ž. Pastuović [b], M. Jakšić [b], Á.Z. Kiss [a]

[a] Institute of Nuclear Research of the Hungarian Academy of Sciences, P.O. Box 51, H-4001 Debrecen, Hungary
[b] Experimental Physics Department, Ruđer Bošković Institute, P.O. Box 180, 10002 Zagreb, Croatia

ARTICLE INFO

ABSTRACT

The spectral deterioration of Hamamatsu S5821 silicon photodiodes for ion types and energies frequently used in Ion Beam Analysis was investigated. Focused proton beams with energies 430 keV and 2 MeV were applied to generate radiation damage via an area selective ion implantation in unbiased diodes at room temperature. The variations of spectroscopic features were measured "in situ" by Ion Beam Induced Current (IBIC) method as a function of fluence, within the 10^9–5×10^{12} ion/cm^2 range and diode bias voltages, between 0 and 100 V.

An empirical model has been developed to describe the radiation damage. Equations are derived for the variations of the normalized peak position and peak width. The derived empirical equations are physically correct, as far as they account for the superposition of the influence of charge carrier trapping by native and radiation-induced defects and for the effect of charge carrier velocity saturation with electric field strength, as well.

1. Introduction

In ion beam applications a semiconductor detector or a device can receive high fluence of energetic (∼MeV) particles directly or indirectly. This is the situation especially in the cases when a device is under study (e.g. a photodiode in our case) in ion beam induced charge microscopy [1], or when a particle detector is used for scanning transmission ion microscopy (STIM) [2,3], respectively. Images are thus based on the contrast of the charge collection efficiency or on the energy loss. In both cases the pulse height amplitude has to be accurately measured for an excellent image quality. In other words, one needs to measure spectral peak position with high accuracy, which requires a good amplitude (energy) resolution of the detecting system.

Since focused beams below 100 nm diameter can be achieved at MeV energies, this poses an ever-increasing demand on the radiation tolerance of the test devices and detectors, as well. For example, an acceptable quality STIM image with such a nano-beam translates to local fluence in the 10^{11}–10^{12} ion/cm^2 range subjected to the silicon detector [2].

As it is known, energetic radiation (especially particles) in semiconductors introduces shallow and primarily deep levels in the forbidden gap. These result in changes of the electric field distribution, change of the capacitance, and primarily, increase of the trapping and generation-recombination probabilities, and thereby increase of leakage current in devices. Consequently, both the charge collection efficiency and the energy resolution deteriorate. The radiation-induced effects, therefore, reduce the quality of the analytical data either in case of IBIC or STIM.

Due to its weak lattice bonding, silicon, together with several other semiconductors, is inherently sensitive to radiation damage [4–6]. An excellent image quality requires excellent statistics, i.e. a well-defined number of incident ions, which combined with the given beam spot size, determines the incident ion fluence directly related to the degree of the damage. The question is therefore, how the charge collection can be improved to minimize the effect of the given radiation damage.

Even in the case of increased trapping and/or recombination probability, the loss of the induced charge can be reduced if the transit time of the generated charge carriers from the generation point to the sensing electrode is minimized. This can be achieved

* Corresponding author. Tel.: +36 52 509 293; fax: +36 52 416 181.
  E-mail address: kalinka@atomki.hu (G. Kalinka).

by shrinking field free regions and increasing the electric field strength in depleted regions, i.e. by applying the highest bias possible.

Since available commercial silicon photodiodes are comparable in their spectral performance to dedicated PIPS (passivated ion implanted planar silicon) nuclear detectors, but are significantly cheaper ($\sim$1 EUR/mm^2), they have been widely used as alternatives [2,3]. It is, therefore, necessary to carry out radiation hardness analysis on such photodiodes, too.

In our previous article [7] we reported no significant spectral deterioration in the photodiodes under study at higher biases due to 2 MeV proton irradiation up to 5×10^{11} ion/cm^2 fluences. An attempt was also made to parameterize the loss of charge collection efficiency (CCE) and energy resolution (FWHM) as a function of fluence and diode bias.

In the present article the spectral effects caused by 430 keV protons in the same diode type are investigated up to 5×10^{12} ion/cm^2 fluences. This is an order of magnitude higher than with 2 MeV protons to introduce approximately the same amount of damage. Now, a more sophisticated evaluation has been applied to the data of the present experiment and of the former one [7], as well, in order to deduce empirical equations for the spectral degradation due to 430 keV and 2 MeV protons. The emphasis is on the drift governed high voltage region, characteristic of particle detector operating conditions.

Note that in our case the radiation damage is rather non-uniform in depth as particles typically fully stop within the detector's sensitive region. In the present experiment the photodiode had a sensitive region of about 100 μm, which can almost be depleted at 100 V reverse bias, while without applied voltage the depleted region is about 3 μm thick [7]. This is to be compared with the ranges of 5 and 50 μm for 430 keV and 2 MeV protons in silicon, respectively.

2. Experimental

Hamamatsu S-5821 Si pin photodiodes (1.2 mm in diameter, typical leakage current 50 pA at room temperature and 3 pF terminal capacitance at 10 V) were used in the recent investigations. Radiation damage was induced by focused 430 keV H$^+$ microbeam scanned over the selected regions of interest. The spectroscopic performance as a function of local particle fluence and applied bias was measured "in situ" with IBIC technique. These measurements were performed at the nuclear microprobe facility of the Ruđer Bošković Institute [8]. The details of the experimental procedure were the same as in our previous work [7].

3. Results and discussion

The distributions of the charge collection deficiency over the patterned irradiation areas obtained as a difference in the median energy values relative to intact, non-irradiated, surrounding regions for both 430 keV and 2 MeV protons at 0 and 100 V bias values are shown in Fig. 1.

The heights of the elevations in 3×3 arrays in the figure show the extent of charge loss caused by *radiation-induced damage*. The rough top of these elevations represents the total charge fluctuation due to charge loss, electronic noises, beam energy instability, etc., i.e. the *total energy resolution*. There are three notable differences between low and high energy proton results: (i) the 0 V/ 100 V charge loss ratio is 10:1 for 430 keV and 25:1 for 2 MeV, (ii) whereas the elevations at 100 V have "sharp" rectangular boundaries in both cases, the 2 MeV data at 0 V are strongly rounded, and (iii) even the non-irradiated surrounding region (partly shown) exhibits a very significant *striped* CCE fluctuation.

As a possible cause, the last effect is related to so-called impurity striations formed during single crystal growth, caused by slight growth rate non-uniformity on a microscopic scale in the melt due to the rotational pulling process [9].

To correct for this effect, true radiation-induced charge losses were calculated by subtracting striation caused background measured prior to irradiation. We note that at higher bias values, when 2 MeV proton tracks are almost within the depletion region, the effect of striations disappears. Namely, striations are observable only during diffusion governed charge collection, when significant fraction of the total ionization energy deposition happens in the field free region. Items (i) and (ii) are also related to the difference in charge collection via drift and diffusion. That is, if in case of mixed collection diffusion plays the dominant role, the charge collection efficiency will be strongly impaired due to recombination. During the slow diffusion process minority charge carriers spend long enough time in the field free region, to diffuse parallel with the collecting electrode" too and thereby "blurring" the IBIC image [7,10].

The effect of diffusion on the charge collection has been separately studied on a virgin diode using 5.5 MeV α-particles from ^{241}Am source, whose projected range is 28 μm at normal incidence and 9 μm at 20° tilt. Somewhat similar to the Diffusion Time Resolved Ion Beam Induced Charge Collection (DTRIBICC) method [11], the distribution of the peaking time T_p, the time between the onset and the maximum amplitude of the unipolar shaped pulses at the output of the linear amplifier, was measured. The delay, ΔT_p, relative to an infinitely fast detector (or pulser) signal caused by nonzero charge collection time is the weighted sum of the drift and diffusion contributions, which – in linear approximation – can be expressed as the first moments of the corresponding current signals, i.e. the mean arrival time of the carriers [12]. Therefore, by varying the depletion depth, w, relative to the projected particle range, the two components can be separated.

By the mean value and the variance of the ΔT_p distribution alike, the experiment proved that the diffusion to drift transition effectively takes place at depletion depths corresponding to the projected particle range, as expected. The mean diffusion time and the relative ballistic deficit [13] caused are maximum at 0 V. For 28 and 9 μm range alphas the mean diffusion times are 65 and 20 ns, while the relative ballistic deficits are 2% and 0.7%, respectively. The mean diffusion distance of the holes during 65 ns is about 9 μm. This is a worst case estimate for the maximum IBIC image blur due to charge collection in this type of diode.

In Fig. 2 the extracted numerical peak position and FWHM data are plotted as a function of the proton fluence. The diffusion and drift dominated regimes are well distinguished. For 2 MeV protons at $U \leqslant 10$ V ($w \leqslant 35$ μm) the diffusion contribution is dominant, whereas for 430 keV protons the diffusion is less pronounced already at 0 V.

For the description of the diffusion driven case there are different approaches [14,15], which show good agreement with the experimental data for not very high fluences ($\leqslant 10^{12}$ ion/cm^2). Since the scope of the present article is the drift dominated case, characteristic of high performance detector regime, we focus on charge carrier loss due to radiation-induced trapping.

However, contrary to the diffusion driven case, no analytical treatment could be found for the drift case, when there is a non-uniform trap distribution within the depletion region. The common assumption is that CCE is practically 100% within the depletion region. This is, however, a rough approximation, as discussed in the thorough treatment of the charge collection due to charged particle induced ionization in the simple case of uniform doping (i.e. linear electric field distribution) and uniform trapping [16–18]. Since neither of these conditions is valid for our diodes, our aim was to find appropriate empirical equations
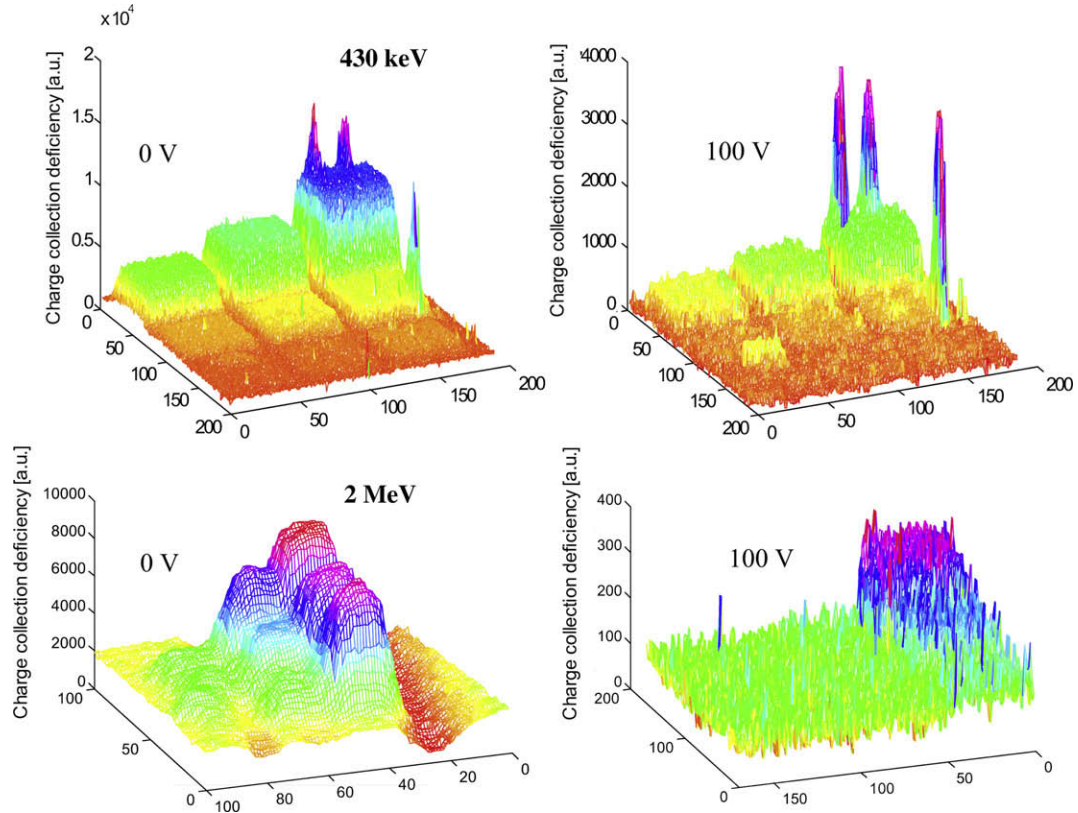
Fig. 1. Irradiation caused charge collection deficiency distributions, relative to neighboring virgin regions for 430 keV and 2 MeV protons at extreme bias values. Note different scales for 0 and 100 V. Giant, random peaks are artifacts due to accidental beam stop during the irradiation process. These regions were excluded from the evaluation. Trenches with 2 MeV protons at 0 V are due, possibly, to growth striations. Their influence on CCE has been corrected for.
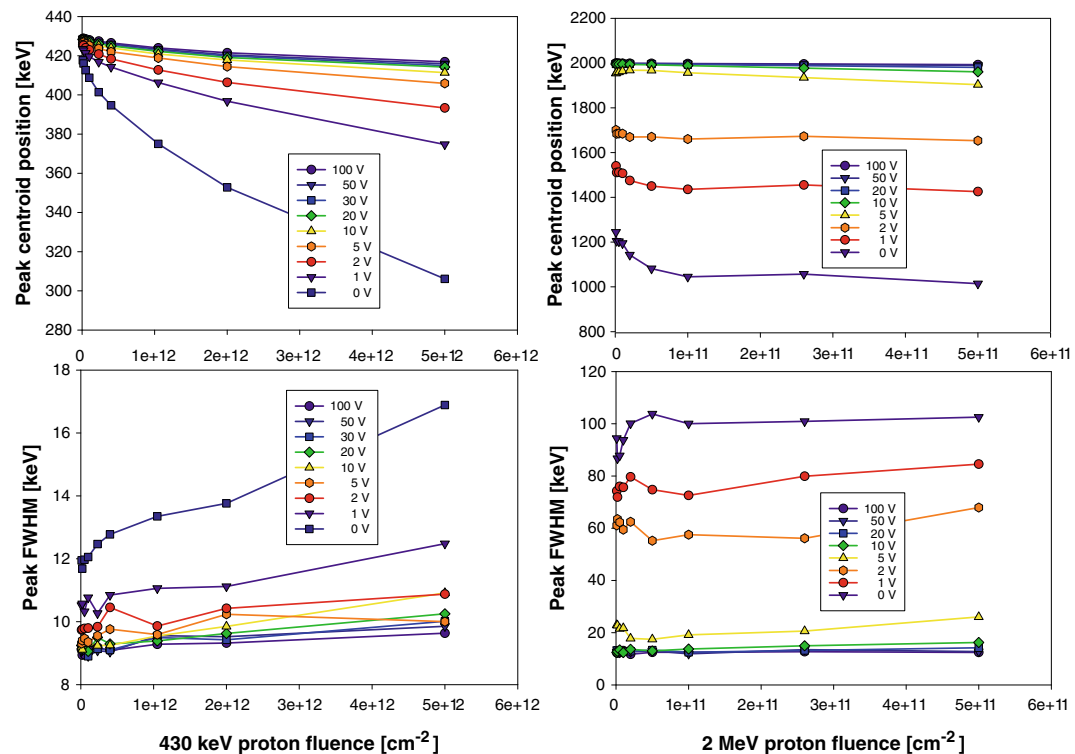

Fig. 2. Summary of peak position (~CCE) and peak width (FWHM) data for 430 keV and 2 MeV protons. Solid lines interconnecting experimental points are intended only to guide the eyes. Please note the difference in the fluence scales.

to quantitatively characterize the actual experimental data for the high voltage region.

The criteria for accepting functional relationships were: (i) linear additivity of charge losses due to native and radiation-induced defects, (ii) squared additivity of independent fluctuations, (iii) evidence for drift velocity saturation, and (iv) relative simplicity. In addition to (i): in the limiting case of no radiation damage, formulas similar to those in [16–18] are envisaged.

Despite relatively large experimental errors, primarily due to electronic noises and weak statistics, a regression analysis of the $P(U, \Phi)$ peak centroid and the FWHM(U, Φ) resolution data sets, taking first the fluence, Φ, then the voltage, U, as independent variable, resulted in fairly reliable equations for the normalized charge loss $\lambda = 1 - CCE$, and its variation, the normalized peak width $\Delta = FWHM/CCE$ (Eqs. (1)–(4)).

$$\lambda_{430} = \left[\varepsilon_{430} + \frac{9.7 \times 10^{-3}}{\sqrt{U}} \right] + \left[1.1 \times 10^{-8} + \frac{2.3 \times 10^{-8}}{\sqrt{U}} \right] \sqrt{\Phi}, \quad (1)$$

$$\lambda_{2000} = \left[\varepsilon_{2000} + \frac{9.0 \times 10^{-3}}{\sqrt{U}} \right] + \left[2.0 \times 10^{-15} + \frac{3.3 \times 10^{-13}}{U} \right] \Phi, \quad (2)$$

$$\Delta^2_{430} = \left[83 + \frac{22}{U} \right] + \left[2.1 \times 10^{-12} + \frac{5.4 \times 10^{-11}}{U} \right] \Phi, \quad (3)$$

$$\Delta^2_{2000} = \left[154 + \frac{3000}{U^2} \right] + \left[8.0 \times 10^{-12} + \frac{1.7 \times 10^{-8}}{U^2} \right] \Phi. \quad (4)$$

Here the charge loss, λ, is expressed in relative units (0–1 range), whereas the squared peak width, Δ^2, in [keV^2], the voltage in [V], and the proton fluence in [ion/cm^2]. Although no detailed error analysis has been carried out, typical errors are estimated to be 10–30%. These expressions are valid in the $0–5 \times 10^{12}$ ion/cm^2 fluence and $U \geqslant 10$ V bias ($w \geqslant 35$ μm) range.

Each of the deduced empirical formulae consists of two main terms separated and enclosed in square brackets. The first bracket terms account for the contribution of the impurities and/or defects already present in the pristine diode material, while the second bracket terms account for the radiation-induced defects. Within each bracket there are again two terms. Each first term is related to the finite saturation value of electron and hole velocities. Namely, they express the charge loss and associated spread due to trapping, which exist in the $U \to \infty$ limit. Using relevant expressions from [16], ε for both energies is in the order of 10^{-4}. Each second term is related to charge losses due to normal trapping and recombination taking place at carrier velocities corresponding to actual detector bias.

The first term in the first bracket for the peak widths (Eqs. (3), (4)) comprises, in addition, the fluctuation of the beam energy, and the deposited energy, due to nonionizing energy losses, and the charge carrier creation (Fano) statistics, and, in our particular case, dominantly electronic noises.

Only a few experimental results have been available in the literature so far on the loss of CCE under similar circumstances, e.g. 10–60 keV energy H$^+$, He$^+$, N$^+$, Ne$^+$ and Ar$^+$ ions on an unbiased Si photodiode, originally with 100% internal CCE, resulted in an exponential decrease with Φ [19]; a PIPS detector irradiated with 4 MeV He$^+$-ions under 60 V operating bias showed a linear decrease up to 4×10^{10} ion/cm^2 fluence [20], another PIPS detector behaved similarly for 2 MeV protons [21]; a Si pin photodiode biased with 10 V exhibited non-linear dependence when irradiated with up to 6×10^{10} and 6×10^{12} ion/cm^2 fluence of 1 MeV He^{2+} and 2 MeV H$_2^+$ ions, respectively [2]. Others found a linear increase of 1/CCE with fluence under very different conditions [22–24].

Our charge collection loss formulae for lower and higher energy protons are the same for the non-irradiated case, but show $U^{-1/2}$ behavior, instead of U^{-1}, as valid for an ideal diode with no significant plasma loss [16–18]. The functional forms at the two energies are, however quite different for the radiation-induced contribu-
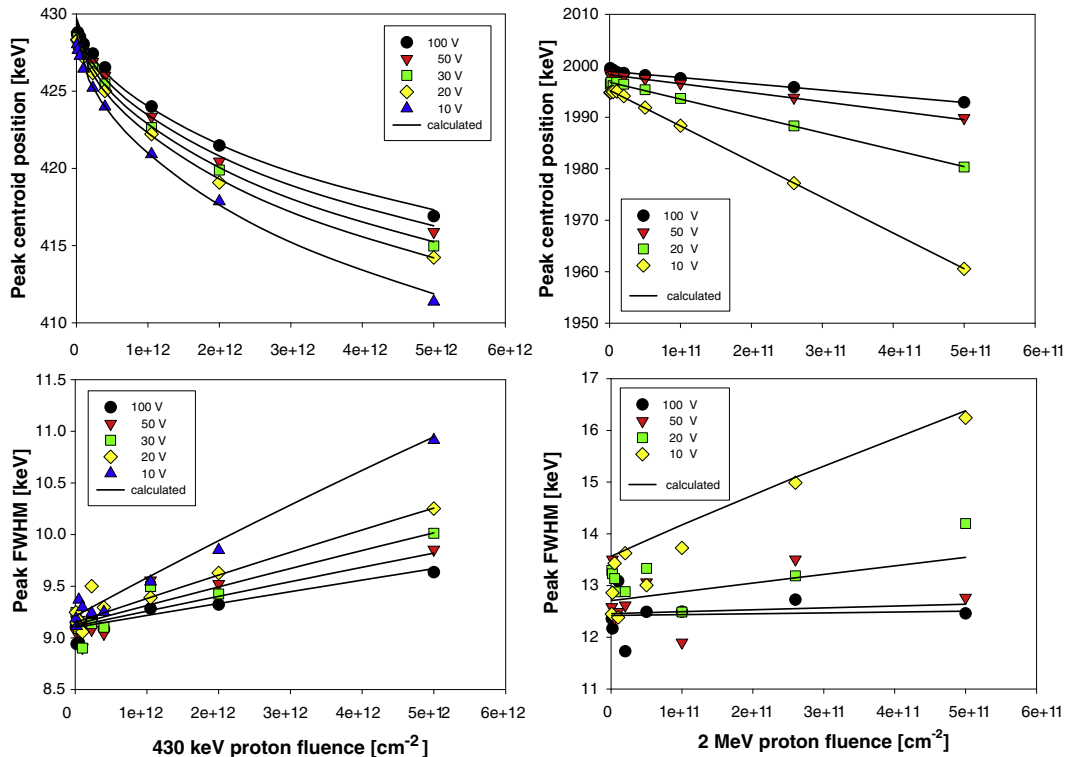

Fig. 3. Comparison of experimental data (symbols) and calculated values (solid lines) of peak positions and peak widths for $U \geqslant 10$ V.

tions, despite critical reassessment of the experimental data. In the lack of similar parameterization there is no reference to compare with our results, so far.

CCE and FWHM values calculated by Eqs. (1)–(4) for voltages from 10 to 100 V together with experimental data are shown in Fig. 3. As evidenced by the figure, the parameterization is excellent for CCE at 2 MeV, still acceptable at 430 keV, but rather weak for FWHM at both energies. Note the much reduced voltage dependence of both CCE and FWHM at 430 keV as compared with 2 MeV data.

4. Conclusions

Radiation-induced damage has been introduced in unbiased Hamamatsu S5821 silicon pin photodiodes by area selective irradiations with 430 keV and 2 MeV proton microbeams within the fluence range of 1×10^9–5×10^{12} ion/cm^2 in logarithmic steps. Radiation-induced spectral response changes of the diodes were measured with IBIC technique with the same beams at different bias voltages within the range of 0 up to 100 V in logarithmic steps, too. Radiation damage decreases the mean value of the peak position in the pulse height spectrum and increases the peak width. By selecting irradiated sub-regions with only homogeneous response, pulse height spectra were extracted, and their "full energy" peak was fitted to a Gaussian. Peak centroids and full width at half maximum values were determined. On the basis of these data sets an empirical model was formed in order to describe the radiation damage effects.

Equations for the normalized shift of the peak position, and for peak width values, as the main quantities used to characterize the spectral performance, were derived for higher bias values, corresponding to the drift dominated charge collection regime. These *empirical* equations are physically correct, as far as they account for the superposition of the charge carrier trapping process of both the native (being already present in the diode without irradiation) and radiation-induced defects, and reflect the effect of charge carrier velocity saturation with electric field strength, as well.

Acknowledgements

References

[1] M.B.H. Breese, E. Vittone, G. Vizkelethy, P.J. Sellin, Nucl. Instr. and Meth. B 264 (2007) 345.
[2] R. Minqin, J.A. van Kan, A.A. Bettiol, D. Lim, C.Y. Gek, B.H. Bay, H.J. Whitlow, T. Osipowicz, F. Watt, Nucl. Instr. and Meth. B 260 (2007) 124.
[3] G. Devès, S. Matsuyama, Y. Barbotteau, K. Ishii, R. Ortega, Rev. Sci. Instrum. 77 (2006) 056102.
[4] H.W. Kraner, IEEE Trans. Nucl. Sci. NS-29 3 (1982) 1088.
[5] V.A.J. van Lint, Mechanisms of Radiation Effects in Electronic Materials, Wiley-Interscience, New York, 1980.
[6] A.G. Holmes-Siedle, L. Adams, Handbook of Radiation Effects, Oxford University Press, 2002.
[7] A. Simon, G. Kalinka, M. Jakšić, Ž. Pastuović, M. Novák, Á.Z. Kiss, Nucl. Instr. and Meth. B 260 (2007) 304.
[8] M. Jakšić, I. Bogdanović Radović, M. Bogovac, V. Desnica, S. Fazinić, M. Karlušić, Z. Medunić, H. Muto, Ž. Pastuović, Z. Siketić, N. Skukan, T. Tadić, Nucl. Instr. and Meth. B 260 (2007) 114.
[9] H.M. Liaw, Crystal growth of silicon, in: W.C. O'Mara, R.B. Herring, L.P. Hunt (Eds.), Handbook of Silicon Technology, Noyes Publications, Park Ridge, 1990, p. 94.
[10] B.L. Doyle, G. Vizkelethy, D.S. Walsh, Nucl. Instr. and Meth. B 161–163 (2000) 457.
[11] B.N. Guo, M. El Bouanani, S.N. Renfrow, M. Nigam, D.S. Walsh, B.L. Doyle, J.L. Duggan, F.D. McDaniel, Nucl. Instr. and Meth. B 181 (2001) 315.
[12] G. Kalinka, ATOMKI Ann. Rep. 2000, p. 66, also at <www.atomki.hu/ar2000/7_develop/d02.pdf>.
[13] B.W. Loo, F.S. Goulding, D. Gao, IEEE Trans. Nucl. Sci. NS-35 (1988) 114.
[14] M.B.H. Breese, J. Appl. Phys. 74 (1993) 3789.
[15] R. Nipoti, C. Donolato, D. Govoni, P. Rossi, G.P. Egeni, V. Rudello, Nucl. Instr. and Meth. B 136–138 (1998) 1340.
[16] N.P. Afanasyeva, E.M. Verbitskaya, V.K. Eremin, N.B. Strokan, E.V. Shokina, LiYaF Preprint No. 1094, August 1985, Leningrad (in Russian).
[17] E.M. Verbitskaya, V.K. Eremin, A.M. Malyarenko, N.B. Strokan, V.L. Sukhanov, B. Schmidt, J. Borany, Phys. Semicond. 27 (1993) 1127.
[18] E. Verbitskaya, V. Eremin, N. Strokan, J. Kemmer, B. Schmidt, J. von Borany, Nucl. Instr. and Meth. B 84 (1994) 51.
[19] S.M. Ritzau, H.O. Funsten, R.W. Harper, R. Korde, IEEE Trans. Nucl. Sci. 45 (1998) 2820.
[20] D.P.L. Simons, A.J.H. Maas, P.H.A. Mutsaers, M.J.A. de Voight, Nucl. Instr. and Meth. B 130 (1997) 160.
[21] M. Maetz, W.J. Przybylowicz, J. Mesjasz-Przybylowicz, A. Schüler, K. Traxel, Nucl. Instr. and Meth. B 158 (1999) 292.
[22] S. Onoda, T. Hirao, J.S. Laird, H. Mori, H. Itoh, T. Wakasa, T. Okamoto, Y. Koizumi, Nucl. Instr. and Meth. B 206 (2003) 444.
[23] I. Nashiyama, T. Hirao, T. Kamiya, H. Yutoh, T. Nishijima, H. Sekiguti, IEEE Trans. Nucl. Sci. NS-40 (1993) 1935.
[24] Ž. Pastuović, M. Jakšić, G. Kalinka, M. Novák, A. Simon, IEEE Trans. Nucl. Sci., submitted for publication.